

CONTROL OF COMBUSTION INSTABILITY USING HELMHOLTZ RESONATOR IN COMBUSTION CHAMBER

Luciana Faria Saint-Martin Pereira

Gabriel Costa Guerra Pereira

Rogério Corá

Pedro Teixeira Lacava

Giuliano Gardolinski Venson

Instituto Tecnológico de Aeronáutica, Praça Marechal Eduardo Gomes, 50, São José dos Campos, SP
 lpereira@ita.br, gpereira@ita.br, cora@ita.br, placava@ita.br, giuliano.venson@unitau.com.br

Abstract. A methodology to empirically validate a Helmholtz resonator design applied to attenuate acoustic oscillations inside a combustion chamber was described. After an estimation of the sound velocity within the combustion chamber, using a software of chemical equilibrium, the resonators were constructed. It was verified if the resonators positioned radially in relation to the chamber would be able to attenuate longitudinal oscillations during combustion, by convenience. The acoustic characterization of the combustion chamber was done with and without the resonator during combustion. They were performed tests with radial and longitudinal resonators individually and with both together. The results showed that the radial resonator has an efficiency of dampen the longitudinal oscillations of 28.8%, however, radial resonator changes abruptly the acoustic characteristics of the chamber, creating an oscillation mode to another frequency (647Hz) not so far from the one that it was designed to attenuate (667Hz). As might be expected, the longitudinal resonator was effective to attenuate the longitudinal oscillation in practically every spectrum of frequency analyzed, with an absorption of 48.2%. The resonators together have attenuated 62.8% at the designed frequency, but did not eliminate the characteristic of the radial resonator of creating a new peak at another frequency (643Hz).

Keywords: combustion instability, Helmholtz resonator of fixed volume; passive control

1. INTRODUCTION

The combustion instability is a phenomenon that accompanies the combustion devices with high rate of energy release as rocket engines, jet engines, gas turbines and industrial burners. The coupling between the combustion process and the pressure oscillations due to acoustic behavior of the combustion chamber may lead to a low efficiency of rocket engines (Santana Jr, 2008).

The oscillatory operation is undesirable because it can be severe and impede the operation of components, achieving structural parts, increase considerably the rate of heat transfer to the chamber walls, melt and destroy parts of the system leading to the explosion of the chamber. Thus, it is necessary to better understand the combustion instability and how to suppress it. Within this context, this work evaluates experimentally the efficiency of acoustic cavities such as Helmholtz resonator to increase the comprehension of acoustic instability and to gain experience in relation to the suppression of this phenomenon.

A cylindrical combustion chamber behaves as an acoustic cavity that may have both longitudinal and transversal acoustic modes (that is, radial and tangential) as well as the combination of these modes. Figure 1(a) shows the pulse of a transversal wave in a spring. Note that the disturbance is perpendicular to the direction of the movement of the wave. Any segment of the spring moves up and down. Figure 1(b) presents the pulse of a longitudinal wave in a spring. The disturbance occurs in the direction of the movement of the wave.

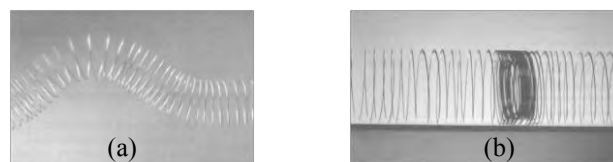


Figure 1. (a) Pulse of a transversal wave in a spring, (b) Pulse of longitudinal wave in a spring.

This work has validated the absorption of longitudinal modes of combustion by performing experiments that use resonators positioned longitudinally and radially in relation to the wall of the combustion chamber, as shown in Fig. 2(a). It was described a methodology to test the effectiveness of the acoustic resonators, because they operate in the chamber as damping systems, which reduces the amplitude of the instability at a particular frequency. The ideal would

be to position the source longitudinally with respect to the combustion chamber, according to Fig. 2(b). However, this possibility was impracticable due to exhaust gases from the combustion which would damage the equipment.

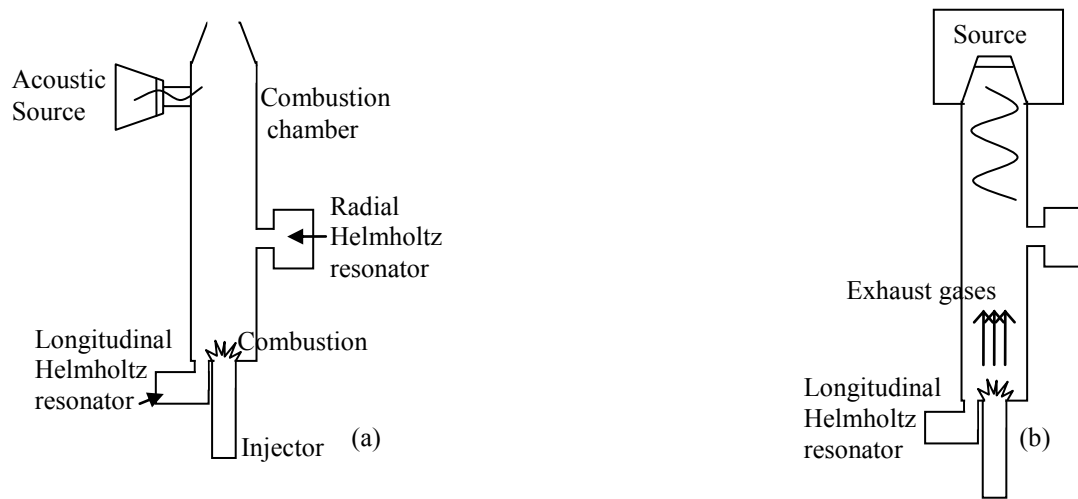


Figure 2. (a) Noise control using longitudinal and radial resonators, (b) Exhaust gases would damage the source.

2. ACOUST TEST ON COMBUSTION CHAMBER

The experimental bench is shown in Fig. 3(a). A sinusoidal acoustic wave, provided by the Function Generator Agilent model 33220A, is amplified by the Sound Amplifier Times One model SL-525 AB4, feeding the Loudspeaker model WPU 1209, manufactured by Selenium, with the membrane diameter of 30.5 mm. The piezoelectric Pressure Transducers Kistler model 7261 measures the pressure fluctuations relative to the average pressure with an accuracy of 2Pa. The electrical signal from the pressure transducer is amplified by the Charge Amplifier Kistler model 5011B. The signals from the piezoelectric transducers, the function generator and the RMS voltage from the loudspeaker were controlled and measured using a data acquisition system, which consists of A Data Acquisition Device, DAQ NI USB 6009, National Instruments, and a Computer, which uses a software acquisition program from LabVIEW 7.0 to present the frequency spectrum and the amplitudes of the pressure within the chamber. Based on the Nyquist criterion, the sampling frequency must be set higher than twice the maximum frequency of interest. In general, the tests were conducted for a frequency range between 500-900 Hz with a resolution of 1Hz and sample rate of 4,000 Hz. The charge amplifiers are adjusted with a sensitivity of 2mbar/volt for all tests. This provided an acceptable resolution for all resonant modes of interest. The pressure transducer was placed at the central position of each module, being X1, X2, X3, X4 and X5. The dimensions of the chamber are on Fig. 3(b), for further information, see Corá (2010).

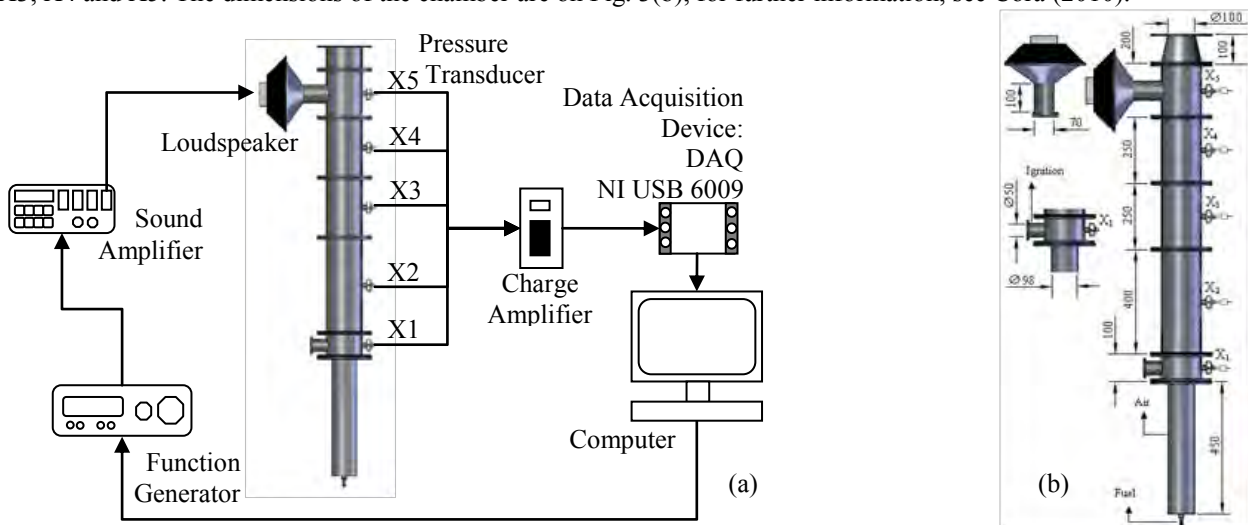


Figure 3. (a) Experimental bench, (b) Combustion chamber dimensions (in mm).

2.1 Resonant Frequencies

A typical spectrum of the model test presented on Fig. 3, in hot gas condition, is shown in Fig. 4. The notations 3L and 4L stand for third and fourth longitudinal mode, respectively. The frequency range observed, that is, from 500 to 900Hz, presented only the 3L and 4L modes. If the frequency range would be higher, for example, from 0 to 20kHz, it would be achieved other modes such as 2T, 3T, 4R, 5R, 2L/1R, 1L / 4T / 3R, among others, being L, R and T the longitudinal, radial and tangential modes, respectively.

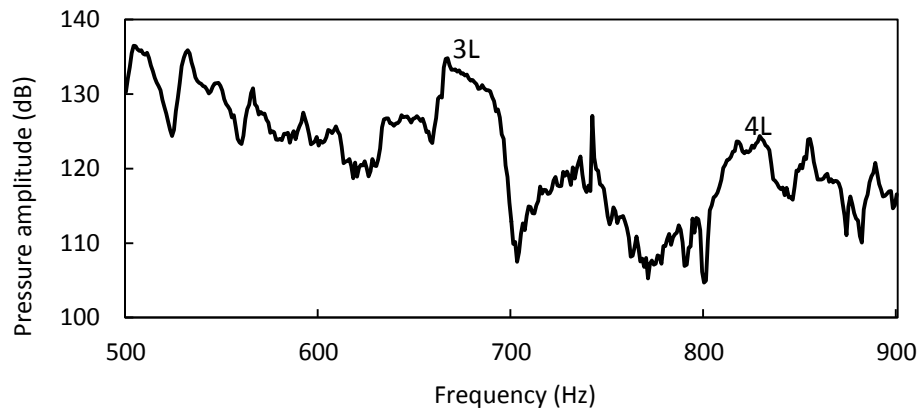


Figure 4. Frequency spectrum measured in the chamber under combustion condition and sine wave noise generation.

Acoustic tests with models have shown that the combustion chamber must be treated theoretically as closed/closed system even though the nozzle is not actually closed (Laudien *at al*, 1995). The eigenfrequencies f_{lmn} (in Hz), or natural frequencies, for a cylindrical chamber closed at both sides can be calculated with Eq. (1),

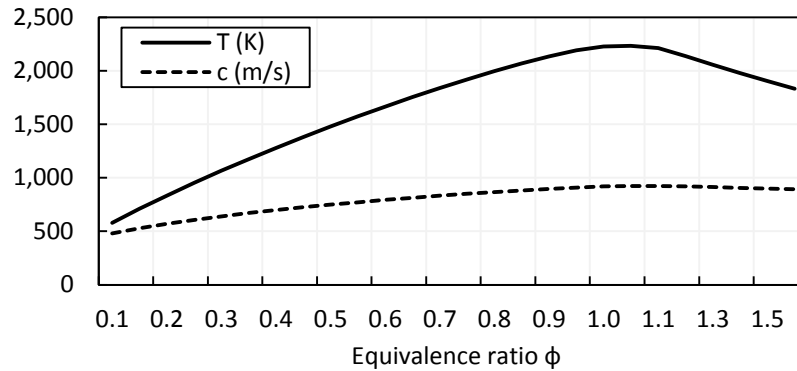
$$f_{lmn} = \frac{c}{2\pi} \sqrt{\left(\frac{\lambda_{lmn}}{R_c}\right)^2 + \left(\frac{l\pi}{L_c}\right)^2} \quad l, m, n = 0, 1, 2, \dots \quad (1)$$

where l, m, n are the longitudinal, tangential and radial mode number, respectively, (dimensionless); c is the velocity of sound (in m/s); λ_{lmn} is the transverse eigenvalue listed in Tab. 1 for the first few modes, (dimensionless); R_c and L_c are radius and length of the combustion chamber, respectively (in m).

Table 1. Transversal eigenvalue (Laudien *at al*, 1995).

n	m					
	0	1	2	3	4	5
0	0	1.8412	3.0542	4.2012	5.3176	6.4156
1	3.8317	5.3314	6.7061	8.0152	9.2824	10.5199
2	7.0156	8.5363	9.9695	11.3459	12.6819	13.9872
3	10.1730	11.7060	13.1704	14.5859	15.9641	17.3128

The variation of the speed of sound will alter the natural frequencies of the acoustic modes in the combustion chamber, as showed in Eq (1). A variation in the combustion equivalence ratio ϕ will alter the temperature of the combustion, and it will change the speed of sound, as showed in Fig. 5 for the methane, estimated by Gaseq. Consequently, the change in the speed of sound will alter the natural frequencies of the acoustic modes in the combustion chamber. The combustion equivalence ratio is defined as the ratio between the number of atoms of oxygen present in the stoichiometric reaction and the number of atoms of oxygen present in the real reaction. Thus, a value of $\phi < 1$ (poor combustion) represents a combustion process with less fuel (or more air) than the stoichiometric case. Otherwise, a value of $\phi > 1$ indicate a rich combustion. (Carvalho Jr and Lacava, 2003)

Figure 5. Variation of the speed of sound as a function of ϕ .

2.2 Helmholtz Resonator

Acoustic cavities such as Helmholtz resonators were successfully used as damping devices for the suppression of combustion oscillations. Resonator consists of a small volume connected with the combustion chamber through an orifice. If the dimensions of the resonator are small in comparison to the wavelength of the oscillation, the gas motion behavior in the resonator is analogous to a mass-spring-damper system (Guimarães *et al*, 2012). The resonant frequency f_0 (in Hz) can be calculated from the geometrical dimensions, showed on Fig. 6, as Laudien *et al* (1995):

$$f_0 = \frac{c}{2\pi} \sqrt{\frac{S}{V(l+\Delta l)}} \quad (2)$$

where S is the cross section of the orifice (m^2), l the orifice length (m), V the cavity volume m^3 , and Δl the mass correction (m), which is (Frendi *et al*, 2005):

$$\Delta l \approx 0.85d \quad (3)$$

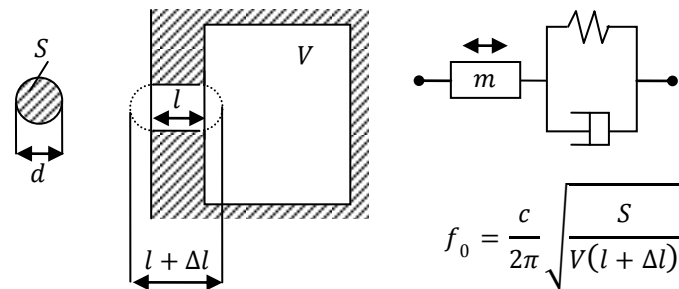


Figure 6. Helmholtz resonator.

To study the acoustical behavior of the resonators, and specially its absorption effect, impedance Z must be determined. This impedance is, in general, a complex unit consisting of the sum of an acoustic resistance R and an acoustic reactance χ :

$$Z = R + i\chi \quad (4)$$

The acoustic impedance is determined by the geometric and mechanical properties of the resonator, in particular the oscillating mass in the orifice, the spring stiffness of the volume and the resistive element associated with viscous dissipation in the orifice. The reactance χ , in $kg/(m^2 \cdot s)$, can be written in terms of the cavity dimensions as Laudien *et al* (1995),

$$\chi = 2\pi f \rho (l + \Delta l) (1 - (f_0^2/f^2)) \quad (5)$$

where f is frequency (Hz) and ρ is density of the combustion gas in the chamber (kg/m^3). The Resistance R , in $kg/(m^2 \cdot s)$, is a function of the orifice length as well as the dynamic viscosity of the gas derived from the combustion, and is defined as Laudien *at al* (1995):

$$R = 4(\varepsilon + l/d)\sqrt{\mu\rho\pi f} \quad (6)$$

where μ is dynamic viscosity of the combustion gas in the chamber, in $Pa \cdot s$, and ε is the resistance factor (dimensionless), which will be discussed later.

When χ and R are multiplied by A/S , one obtains the specific resistance r and reactance x (dimensionless):

$$x = \chi \frac{A}{NS} \quad (7)$$

$$r = R \frac{A}{NS} \quad (8)$$

where A is the cross-sectional area of the combustion chamber (m^2), S the cross cross-sectional area of the orifice (m^2) and N is the number of the tuned absorbers around the circumference of the combustion chamber. Once the impedance is known, the absorption coefficient α and the conductance ξ (real part of the admittance) can be evaluated as Laudien *at al* (1994):

$$\alpha = \frac{4r}{\rho c} \left[\left(1 + \frac{r}{\rho c}\right)^2 + \left(\frac{x}{\rho c}\right)^2 \right] \quad (9)$$

$$\xi = \frac{r}{\rho c} \left[\left(\frac{r}{\rho c}\right)^2 + \left(\frac{x}{\rho c}\right)^2 \right] \quad (10)$$

The calculation of the resistance factor ε is not very clear in the literature. Several bibliographies were searched and noted that the author that more addresses this issue is Ingard. Ingard (1953) presented in his work a parameter called hole parameter $h(l/r_o)$ that is plotted in function of ε according to Fig. 7 for different values of l/r_o :

$$h(l/r_o) = \frac{(\beta + 0.59l/r_o)^2}{(\varepsilon + 0.5l/r_o)} \quad (11)$$

The role parameter refers to the orifice of the Helmholtz resonator, where l and r_o are the length and the radius of the orifice.

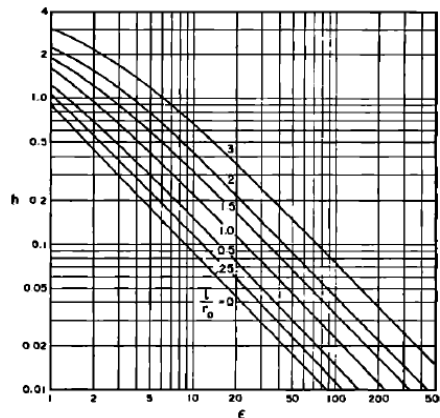


Figure 7. The hole parameter h presented as a function of ε , with l/r_o as parameter.

Starting from the initial condition that $\varepsilon = 1$ and $\beta = 0.9$, according to Ingard (1953), the equation above becomes:

$$h(l/r_o) = \frac{(0.9 + 0.59l/r_o)^2}{(1 + 0.5l/r_o)} \quad (12)$$

As $l/r_o = 5$ for this work, the value of h is approximately 4. Extrapolating the curve l/r_o to the value 5 in Fig. 7, it was considered that $\varepsilon \approx 20$.

2.3 Frequencies of Combustion Instability

Combustion instabilities have been classified in two major categories: high-frequency instability and low-frequency instability (Santana Jr., 2008). According to Pikalov (2001), the frequencies are classified as low-frequency when the wavelength of the pressure oscillation (λ_0) is much larger than the dimensions of the chamber and as high-frequency when the wavelength is approximately equal or smaller than chamber length.

$$\lambda_0 = c/f_0 \quad (13)$$

2.4 Positioning of The Resonator

The resonator should be positioned in the region of greatest pressure amplitude. Thus, it is important to know the pressure response in a slender duct closed at both sides, similar to the one of this study, which can be given by Beranek and Vér (1992):

$$\psi_j = \cos \frac{j\pi z}{L_c} \quad j = 0,1,2, \dots \quad (14)$$

where ψ is the mode amplitude (dimensionless), z is the displacement along the chamber length (in m) and j is the acoustic mode (dimensionless).

3. RESULTS

The Nyquist Frequency for this experiment is equal to 2×900 Hz, that is, 1,800 Hz. This is equivalent to 1,800 samples per second, or 1.8 kS/s. The DAQ NI USB-6009 has used his 48 kS/s divided by 8 channels (being them 7 channels that connect the sensors plus 1 channel that connect the transducer). Thus, 48 kS/s divided by 8 channels is equal to 6 kS/s for each channel. That is, 6 kS/s is much greater than the Nyquist frequency of 1.8 kS/s, and therefore, the DAQ satisfies the Nyquist criterion for this experiment, thus avoiding the aliasing.

The 7 sensors are sensors of temperature, pressure and pressure variation, both for fuel and oxygen, plus a sensor of atmospheric pressure. These sensors were used to enter the data into a LabView program that calculates the fuel mass flow and oxygen mass flow, through orifice plate system.

Table 2 compares the natural frequencies calculated using Eq. (1) with those frequencies measured experimentally through the chamber, using the pressure transducer, showing agreement between them, with an error less than 1%.

Table 2. Natural frequencies of acoustic modes in the combustion chamber.

Mode	Theoretical Frequency (Hz)	Experimental Frequency (Hz)	Error (%)
3L	634	630	0,67
4L	845	845	0,04

The resonators were designed to absorb at the frequency of third longitudinal mode, with combustion. It was used the adiabatic temperature of flame for $\phi = 0.15$ (see Fig. 8). To calculate the theoretical values of Tab. 2 it was used the speed of sound from Tab. 3, which was obtained through a program of chemical equilibrium, called Gaseq. For simplification, the temperature was considered uniform throughout the chamber, but in reality case, this is not true.

Table 3. Data estimated from Gaseq, 2005.

Input Data	
Problem Type	Adiabatic T and composition at Constant P
Reactants	Methane/air flame
Stoichiometric, Phi	0.15
Output Data	
T = 709,3K	Temperature inside the camera
c = 528.2 m/s	Speed of sound
$\rho = 0.4923 \text{ kg/m}^3$	Density of the gas in the combustion chamber
$\nu = 3.38 \times 10^{-5} \text{ Pa.s}$	Dynamic viscosity of the gas in the combustion chamber

For the selection of the equivalence ratio, they were made tests with different values of equivalence ratio using methane (CH₄) as fuel, in order to select the one of highest pressure amplitude in both cases showed on Fig. 8:

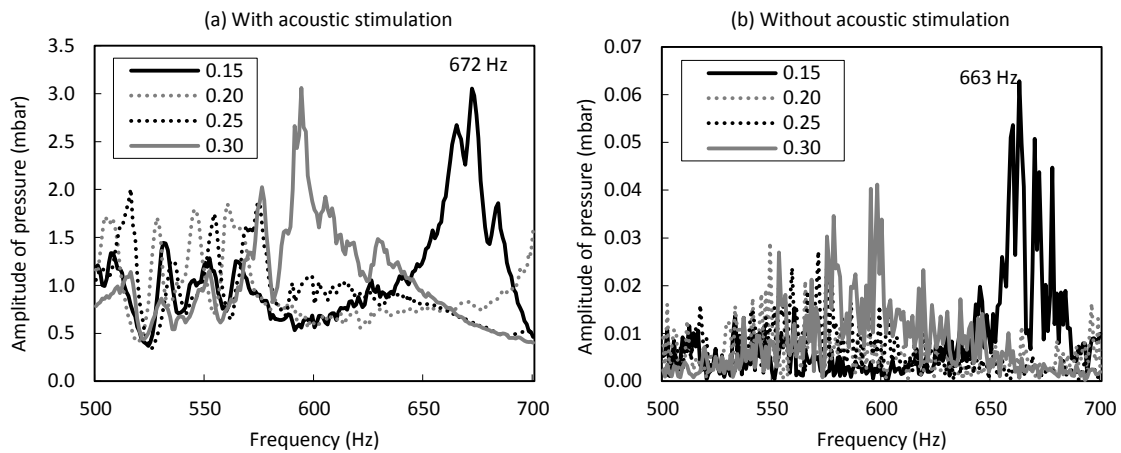


Figure 8. Combustion with different equivalence ratios, (a) with and (b) without acoustic stimulation.

From the Tab. 4, it can be noted that the frequencies of the combustion instability can be classified as high-frequency once the wavelength $\lambda_0 = 0.792\text{m}$ is smaller than the chamber length $L_c = 1.250\text{m}$.

Table 4. Dimensions of combustion chamber.

Input Data	Extracted From
$R_c = 0.075\text{m}$	Measured in chamber
$L_c = 1.250\text{m}$	Length of the combustion chamber

Figure 9 shows that the behavior of the pressure amplitude is the same with and without acoustic stimulation, but with acoustic stimulation the curve of the pressure amplitude is amplified in approximately 100 times. This curve was extracted at the position X1. The other positions have similar behavior.

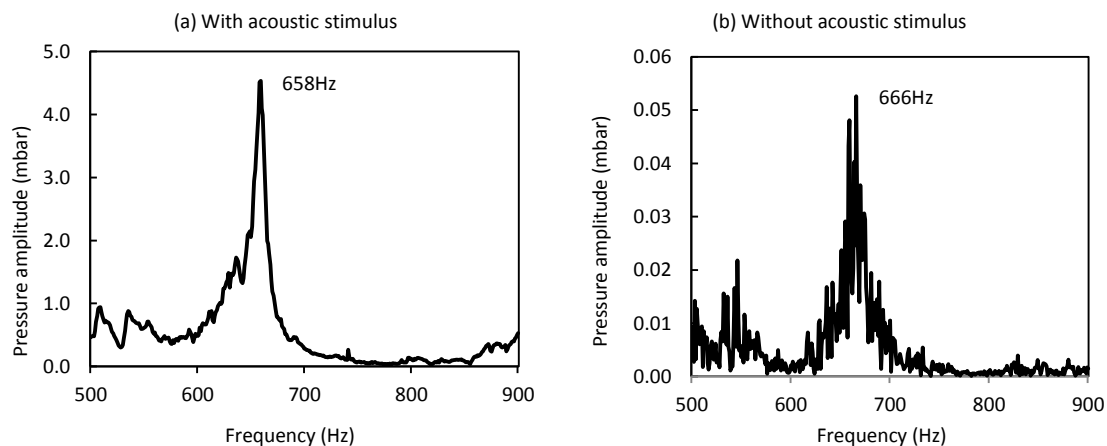


Figure 9. Test with combustion, (a) with and (b) without acoustic stimulus at X1 position.

The value of f_0 was obtained experimentally, according to the Fig. 10, being so $f_0 = 667\text{Hz}$. The others values were calculated according to Tab. 5. It was made an analysis of acoustic characteristics of the chamber with combustion, according to Fig. 10, that shows the pressure amplitudes, with the pressure transducer in positions from X1 to X5, with combustion equivalence ratio equal to 0.15, with and without acoustic stimulus. Note that the pressure amplitudes are amplified with acoustic stimulus and that in both cases there are highest frequencies close to 667 Hz.

L. Pereira, G. Pereira and R. Corá
Control of Combustion Instability in Combustion Chamber

Table 5. Helmholtz resonator design.

Output Data	Extracted From
$S = 1.13 \times 10^{-4} \text{m}^2$	$S = \pi d^2/4$
$V = 4.5 \times 10^{-5} \text{m}^3$	Eq. (2)
$\Delta l = 0.010 \text{m}$	Eq. (3)
$A = 1.77 \times 10^{-2} \text{m}^2$	$A = \pi R_c^2/4$

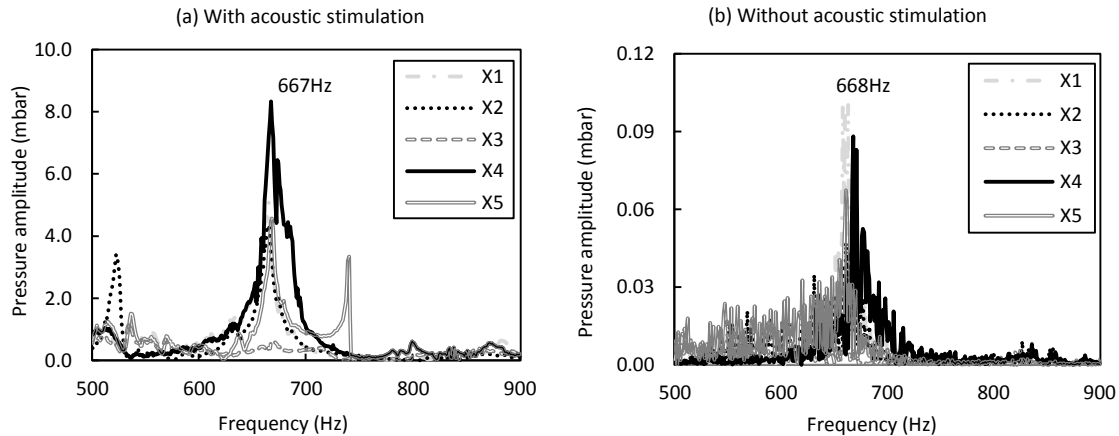


Fig. 10: Frequencies from X1 to X5, with $\phi = 0.15$, for the choice of f_0 (a) with acoustic stimulation and (b) without acoustic stimulation.

The dimensions of the resonator are small in comparison to the wavelength of the oscillation, once the largest dimension, which is D , represents less than 10% of λ_0 , as showed on Tab. 6. Thus, the gas motion behavior in the resonator is analogous to a mass-spring-damper system.

Table 6. Dimensions of the designed Helmholtz resonator.

Dimensions	Percentage of λ_0
$d = 0.012 \text{m}$	1.5%
$l = 0.030 \text{m}$	3.8%
$D = 0.053 \text{m}$	6.7%
$L = 0.020 \text{m}$	2.5%
$\lambda_0 = 0.792 \text{m}$	-

The absorption coefficient has its optimum at 100%, while the conductance, by definition, has no limitation. Figure 11 shows the spectral behavior of the absorption coefficient as well as the conductance for three different absorber arrangements in a closed tube. If the system had the damping optimized taking into account only the absorption coefficient, would be suggestive to choose the arrangement with higher absorption, that is, with 12 resonators. On the contrary, if taken into account the maximization of the conductance, the best configuration would be 24 or more resonators. Acoustically speaking, more than 12 resonators overdamp this system, which implies in less than 100% absorption, but increase the width of the frequency band absorbed. The most usual approach is to optimize the damping by the absorption coefficient, despite the uncertainties of this model due to the non homogeneity of the field of acoustic pressure (Laudien *et al.*, 1994). Thus, it was decided to the arrangement of 12 resonators.

Figure 12 shows the locations of nodes and anti-nodes, extracted from Eq. (14), the 5 positions of the pressure transducers by a black circle, as well as the location of the 2 rows of the radial resonator by a triangle.

In the position $z = 0.000 \text{m}$ the amplitude is maximum and so, at this point the longitudinal resonator was coupled. The ideal would be to couple all radial resonators in a position where the amplitude is maximal, that is, in an anti-node (Tab. 7).

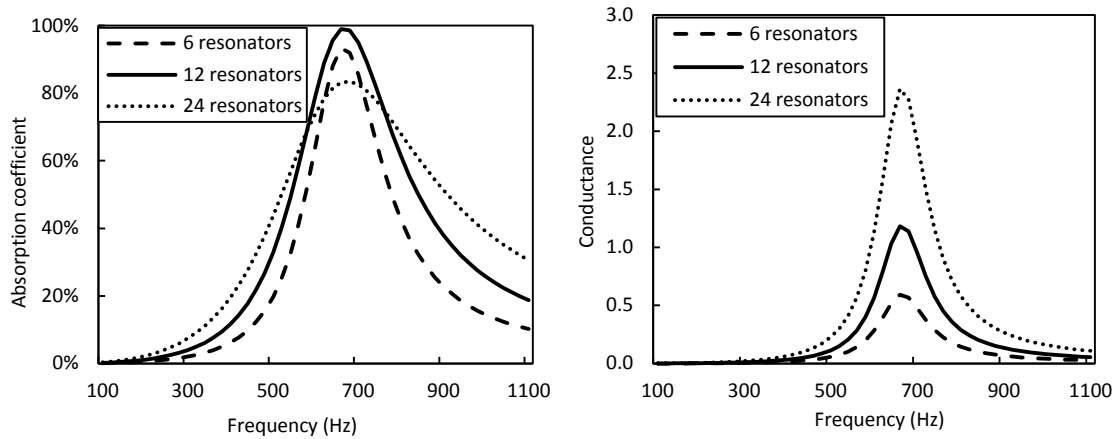


Figure 11. Absorption behavior of an under (6), optimized (12) and overdamped (24) system.

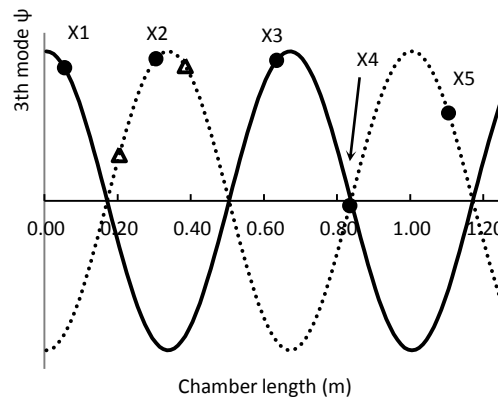


Figure 12. Choosing the position of the resonator.

Table 7. Node and anti-node positions.

Node position (z)	3 th Mode	4 th Mode	Anti-node position (z)	3 th Mode	4 th Mode
		0.160		0.130	
	0.500	0.380		0.330	0.250
	0.830	0.620		0.670	0.500
	1.170	0.870		1.000	0.750
	-	1.120		-	1.000
	-	-		-	1.250

However, the radial resonators were coupled in two rows (Fig. 13) to avoid physical interference between them. Thus, the radial resonators were positioned in $z = 0.200$ m (very close to a node, that is, where the amplitude is zero, and there is no pressure to absorb) and $z = 0.400$ m, at 75% of the maximum amplitude, as showed on Fig 12. Nevertheless, the chamber is not completely closed-closed because the upper side has an aperture of 30% of the diameter of the chamber in order to exhaust the combustion gases. Thus, the curve might change and therefore the position of the node shall shift slightly. Furthermore, there is a cooling device between the rows of the radial resonators, showed on Fig. 13(b). Although the resonators have different geometries, the volumes of both are the same. Both radial and longitudinal resonators have fixed volume. The resonators were coupled in two configurations, being them, radial resonator, positioned in the wall of the combustion chamber and, longitudinal resonator positioned in the injector. Tests were performed with radial and longitudinal resonators individually, and then, with both resonators together.

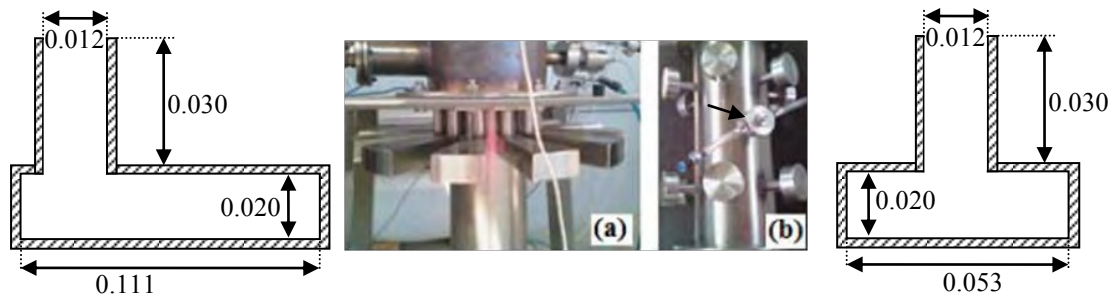


Figure 13. (a) Longitudinal and (b) radial resonator coupled to the chamber.

Figure 14 shows the amplitudes of pressure for the transducer at the 5 different positions that were presented in Fig.3, at the same scale of pressure amplitude:

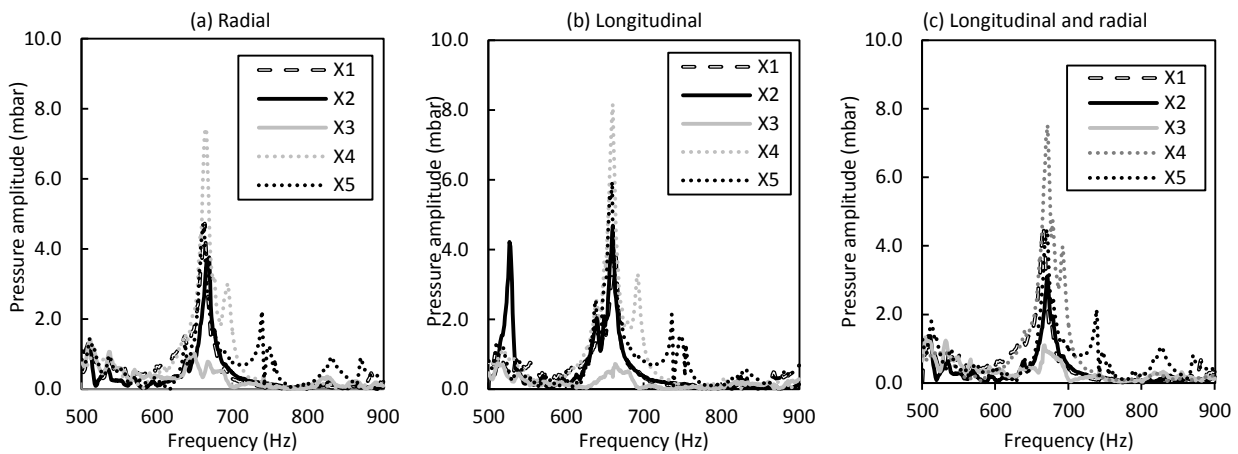


Figure 14. Results with (a) radial, (b) longitudinal, and (c) radial with longitudinal resonators, on 5 different positions.

The highest amplitudes of each position are listed on Tab 8. It may be noted, for both configurations of the radial and longitudinal resonators, that the smaller amplitudes appeared at X3, whereas the greatest amplitudes appeared at X4. By this observation, it could be concluded that X3 is near a node whilst X4 is near an anti-node. However, when comparing these results with those from Fig. 12, it is noted that X3 is close to an anti-node and that X4 is near a node (see Tab. 7). It may be influence of the node near X3 for the 4th mode. Therefore, the approximation that uses the equation of closed-closed tube, Eq. (1), may not be adequate to determine where the nodes and anti-nodes are. Probably, a numerical analysis of finite elements may give a more accurate result of these positions.

Table 8. Highest pressure amplitudes in each position, in mbar.

	X1	X2	X3	X4	X5
Radial highest amplitudes (mbar)	4.7	3.8	1.4	7.4	4.7
Longitudinal highest amplitudes (mbar)	4.1	4.7	0.8	8.2	5.9
Radial and longitudinal highest amplitudes (mbar)	4.6	3.1	1.5	7.5	4.5
Transistor position (m)	0.050	0.300	0.625	0.875	1.100

Table 9 shows how the resonators have absorbed, in each position, for the frequency in which they were designed to absorb (667Hz). With the use of the resonators radial and longitudinal, it was expected that there would be a reduction in the amplitude compared to the situation without resonator. However, it was observed that there was absorption of the pressure amplitude for certain positions and amplification for others.

Figure 15 shows the best result for the (a) radial resonator, (b) longitudinal resonator and (c) both resonator together, compared with the curve without the resonator. The position X3, showed the best result for all cases, at the frequency of 667Hz, being them: 28.8% of absorption for radial resonator, 48.2% for longitudinal resonator and, 62.8% for both together.

Table 9. Amplitudes in 667 Hz for each position.

	X1	X2	X3	X4	X5
Without resonator (mbar)	1.8	2.7	1.1	2.9	3.4
With radial resonator (mbar)	2.8	3.6	0.8	6.3	2.7
With longitudinal resonator (mbar)	2.5	1.8	0.6	3.4	2.2
With radial and longitudinal resonator (mbar)	4.1	2.2	0.4	6.2	4.0

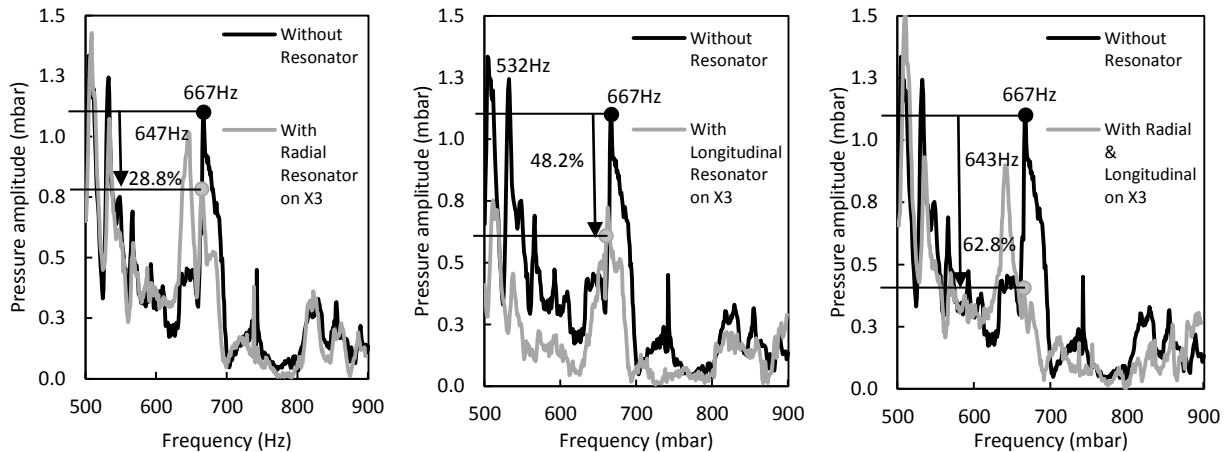


Figure 15. Best results for (a) radial, (b) longitudinal and (c) radial and longitudinal resonators.

It is noted on Fig. 15(a) that the radial resonator creates a local action of dampen the oscillations at the frequency of design (667Hz) but, on the other hand, has little effect of damping on other frequencies and changes the acoustic behavior of the chamber, creating a new peak near the frequency of 647 Hz. It is also noted on Fig. 15(b), that the longitudinal resonator attenuates with greater intensity the oscillation in the frequency of design (667Hz), and, in addition, also attenuated the remaining frequencies of the spectrum studied, especially for the damping at 532 Hz. The Fig. 15(c) shows the results of tests with two resonators together. The association of the two resonators demonstrated to be very beneficial for the frequency of project (667Hz); decreasing significantly the oscillation amplitude (62.8%) compared with the isolated resonators (being them: 28.8% for radial and 48.2% for longitudinal). However, the influence of the radial resonator in change the acoustic characteristics of the combustor can be observed again, appearing a peak in the frequency of 643 Hz. This peak is slightly attenuated in relation to the situation of the radial resonator isolated, probably by the action of the longitudinal resonator. The advantage of to attenuate the entire spectrum obtained for the longitudinal resonator isolated was not observed when the two resonators are absorbing together.

4. CONCLUSIONS

The present work has established a mathematical formulation to design resonators for control of acoustic instabilities with possible application in liquid propellant rocket engines. Based on this methodology, two systems were designed, built and tested, longitudinal and radial resonators

The idea was to determine whether a radial resonator has the ability to attenuate longitudinal oscillations generated during the combustion, because in case of rocket systems, for example, it would be much more convenient to position the resonators in the wall of the combustion chamber than in the injector of propellants, as would be in the case of longitudinal resonators.

The results show that the radial resonator alone has an efficiency of dampen the longitudinal oscillations of 28.8%, which is smaller than the longitudinal resonator, of 48.2%. However, radial resonator changes abruptly the acoustic characteristics of the chamber, creating one oscillation mode to another frequency (647Hz) not so far from the one that it was designed to attenuate (667Hz).

As might be expected, the longitudinal resonator was effective to mitigate the oscillations in practically every spectrum of frequency analyzed. The combination of the resonators was positive, attenuating in 62.8% the frequency of project (667Hz), but did not eliminate the characteristic of the radial resonator of to create a new peak at another frequency (643Hz) next to the one of the project (667Hz).

L. Pereira, G. Pereira and R. Corá
Control of Combustion Instability in Combustion Chamber

5. REFERENCES

- Beranek, L., Vér, I., 1992. *Noise and Vibration Control Engineering*. John Wiley & Sons, Toronto.
- Carvalho Jr, J. A. and Lacava, P. T., 2003. *Emissões em Processos de Combustão*. Unesp Publishing House, p.87.
- Corá, R., 2010. *Controle Passivo de Instabilidades de Combustão Utilizando Ressonadores de Helmholtz*. Ph.D. thesis, Instituto Tecnológico de Aeronáutica, São José dos Campos.
- Freñdi, A., Nesman, T. and Canabal, F., 2005. "Control of Combustion-Instabilities Through Various Passive Devices". In *Proceedings 11th AIAA/CEAS Aeroacoustics Conference - ARC2005*. New York.
- GASEQ, 2005. "Chemical Equilibrium Program in Perfect Gases", v. 0.79. Sep. 2013 <<http://www.gaseq.co.uk/>>.
- Guimarães, G. P., Pirk, R., Souto, C. D., Rett, S. R. and Góes, C. S., 2012. "Acoustic Modes Attenuation on Rocket Engines Using Helmholtz Ressonators: Experimental Validation". In *Proceedings of the 15th International Conference on Experimental Mechanics - ICEM2012*. Porto, Portugal.
- Ingard, U., 1953. "On The Theory and Design of Acoustic Resonators." *The Journal of The Acoustical Society of America*, Vol. 25, n. 6.
- Langel G., Laudien E., Pongratz R. and Habiballah M., 1991. "Combustion Stability Characteristics of the Ariane 5 L7 Engine". In *Proceedings of the 42nd Congress of the International Astronautical Federation - IAC1991*. Montreal, Canada.
- Laudien E., Pongratz R., Pierro R. and Preclik D., 1994. "Experimental Procedures Aiding the Design of Acoustic Cavities". *Liquid Rocket Engine Combustion Instability*. Progress in Astronautics and Aeronautics, Vol. 169, p. 377-399.
- Santana Jr., A., 2008. *Investigation of Passive Control Devices to Suppress Acoustic Instability in Combustion Chambers*. Ph.D. thesis, Instituto Tecnológico de Aeronáutica, São José dos Campos.
- Pikalov, V. P. and Dranovski, M. L., 2001. *General Principles to Evaluation of High-frequency Combustion Instability in Liquid Rocket Engines*. Russia.

6. RESPONSIBILITY NOTICE

The author(s) is (are) the only responsible for the printed material included in this paper.